Cell Research (2017) 27:1034-1045.

www.nature.com/cr

ORIGINAL ARTICLE

Inhibition of the B7-H3 immune checkpoint limits tumor growth by enhancing cytotoxic lymphocyte function

Young-hee Lee[1, *], Natalia Martin-Orozco[1, 11, *], Peilin Zheng[4, 9, 10], Jing Li[7], Peng Zhang[12], Haidong Tan[13], Hyun Jung Park[5], Mira Jeong[6], Seon Hee Chang[1], Byung-Seok Kim[1], Wei Xiong[9, 10], Wenjuan Zang[7], Li Guo[14], Yang Liu[12], Zhong-jun Dong[7], Willem W Overwijk[2], Patrick Hwu[2], Qing Yi[3, 15], Larry Kwak[3, 16], Zhiying Yang[13], Tak W Mak[8], Wei Li[5], Laszlo G Radvanyi[2, 11], Ling Ni[7], Dongfang Liu[4, 9], Chen Dong[7]

[1]Department of Immunology, [2]Department of Melanoma, [3]Departments of Lymphoma and Myeloma, U.T. MD Anderson Cancer Center, 7455 Fannin St., Houston, TX 77054, USA; [4]Center for Inflammation and Epigenetics, Houston Methodist Research Institute, 6670 Bertner Ave, Houston, TX 77030, USA; [5]Department of Molecular and Cellular Biology, [6]Department of Pathology and Immunology, Baylor College of Medicine, Houston, TX 77030, USA; [7]Institute for Immunology and School of Medicine, Tsinghua University, Beijing, 100084, China; [8]The Campbell Family Institute for Breast Cancer Research at Princess Margaret Cancer Centre, Ontario Cancer Institute, University Health Network, Toronto, ON M5G 2M9, Canada; [9]Department of Microbiology and Immunology, Weill Cornell Medical College, Cornell University, New York, NY 10065, USA; [10]The Second Xiangya Hospital, Central South University, Key Laboratory of Diabetes Immunology, Ministry of Education, National Clinical Research Center for Metabolic Diseases, 139 Renmin Road, Changsha, Hunan 410011, China; [11]EMD Serono Research and Development Institute, Inc. 45A Middlesex Turnpike, Billerica, MA 01821, USA; [12]Center for Cancer and Immunology Research, Children's National Health System, Washington DC, 20010 USA; [13]Department of Hepatobiliary Surgery, China-Japan Friendship Hospital, Beijing, 100029, China; [14]X-KANG United Biopharmaceutical Science & Technology Co. Ltd., Suzhou, Jiangsu 215000, China; [15]Department of Cancer Biology Betsy B. DeWindt Endowed Chair for Cancer Research, Lerner Research Institute, Cleveland Clinic, 9500 Euclid Avenue, Cleveland, OH 44195, USA; [16]City of Hope National Medical Center, 1500 East Duarte Road, Duarte, CA, 91010, USA

The interaction between tumor and the immune system is still poorly understood. Significant clinical responses have been achieved in cancer patients treated with antibodies against the CTLA4 and PD-1/PD-L1 checkpoints; however, only a small portion of patients responded to the therapies, indicating a need to explore additional co-inhibitory molecules for cancer treatment. B7-H3, a member of the B7 superfamily, was previously shown by us to inhibit T-cell activation and autoimmunity. In this study, we have analyzed the function of B7-H3 in tumor immunity. Expression of B7-H3 was found in multiple tumor lines, tumor-infiltrating dendritic cells, and macrophages. B7-H3-deficient mice or mice treated with an antagonistic antibody to B7-H3 showed reduced growth of multiple tumors, which depended on NK and $CD8^+$ T cells. With a putative receptor expressed by cytotoxic lymphocytes, B7-H3 inhibited their activation, and its deficiency resulted in increased cytotoxic lymphocyte function in tumor-bearing mice. Combining blockades of B7-H3 and PD-1 resulted in further enhanced therapeutic control of late-stage tumors. Taken together, our results indicate that the B7-H3 checkpoint may serve as a novel target for immunotherapy against cancer.

***Keywords*:** B7-H3; checkpoint inhibition; tumor immunity; immunotherapy

Cell Research (2017) **27**:1034-1045. doi:10.1038/cr.2017.90; published online 7 July 2017

Introduction

T-cell tolerance is controlled by a combinatorial co-stimulation signal. Whereas CD28 and ICOS (inducible T-cell co-stimulator) are important in T-cell activation or function, negative co-stimulation, or co-inhibition, maintains the threshold of T-cell activation [1, 2]. Increasing evidence indicates that these co-inhibitory molecules, such as PD-1 (programmed death 1) and its ligand PD-

*These two authors contributed equally to this work.
Correspondence: Chen Dong
E-mail: chendong@tsinghua.edu.cn
Received 18 September 2016; revised 3 May 2017; accepted 25 May 2017; published online 7 July 2017

L1 (aka B7-H1, B7 homolog 1), are present in the tumor microenvironments and help tumor cells to evade immune destruction [3]. Blockade of PD-L1 alleviated suppression of tumor immunity mediated by myeloid dendritic cells (mDCs) through regulation of cytokine production [4]. Anti-CTLA4 and anti-PD-1 antibody treatments have shown clinical efficacy in cancer patients [5-7], highlighting a new pathway for tumor immunotherapy [8]. However, not all patients or cancer models respond to these checkpoint inhibitors. For example, we previously found that anti-PD-L1 was not effective in promoting tumor regression in the B16 melanoma model [9], suggesting that additional pathways ought to be studied to achieve optimal tumor immunity.

B7-H3 (CD276) is one of the B7 superfamily molecules [10, 11]. In mice, B7-H3 is constitutively expressed on professional antigen-presenting cells (APCs) and gets upregulated on DCs after activation with lipopolysaccharide (LPS) [12]. B7-H3 co-inhibitory function was described using a B7-H3-Ig fusion protein, where it decreased proliferation, and interleukin-2 (IL-2) and interferon-γ (IFN-γ) production by T cells activated with anti-CD3 [12, 13]. Moreover, B7-H3 gene deletion or blockade with an antibody enhanced experimental autoimmune encephalomyelitis [12, 13]. In humans, B7-H3 was first reported in DCs as a positive co-stimulator that enhanced IFN-γ production during T-cell activation [10]. However, more recently, a study showed potent inhibition of IFN-γ, IL-2, IL-10, and IL-13 production during T-cell activation [14]. So far the receptor for B7-H3 has not been identified.

In cancer patients, B7-H3 expression was previously identified as a poor prognostic factor. For example, B7-H3 expression in non-small cell lung cancer patient is associated with an advanced tumor stage, tumor size, and lymph node metastasis [15, 16]. In carcinomas, B7-H3 expression in tumors correlated with shorter survival time and higher cancer recurrence [17]. Although these and other studies implicate a role for B7-H3 in human cancers, the underlying mechanism of B7-H3 function in cancer has remained unclear.

In the current study, we have analyzed the role of B7-H3 in murine cancer models. We found that B7-H3 was expressed in the tumor microenvironment of mouse and human tumors. B7-H3 inhibition controlled tumor growth and anti-tumor immunity was dependent on $CD8^+$ T cells and natural killer (NK) cells. Moreover, B7-H3 directly inhibited the activation of NK cells. Thus, B7-H3 serves as a critical negative regulator in tumor immunity and could in principle be targeted in cancer immunotherapy.

Results

Expression of B7-H3 and its receptor in human and murine tumors

As a first step to analyze the role of B7-H3 in cancer immunology, we determined the expression of B7-H3 in cancer patients. Analysis of The Cancer Genome Atlas (TCGA) data revealed that transcripts of B7-H3 were upregulated in multiple types of tumors in comparison with matched normal tissues (Supplementary information, Figure S1). We also tested the mRNA and protein levels of B7-H3 in biopsies from patients with hepatocellular carcinoma (HCC) or melanoma. In HCC patients, expression of B7-H3 on $CD14^+HLA\text{-}DR^{hi}$ macrophages, $CD14^+HLA\text{-}DR^{low/-}$ monocytic myeloid-derived suppressive cells, and mDCs was upregulated in the liver compared with the peripheral blood, whereas APCs in the tumor possessed even higher B7-H3 expression than in the normal liver or para-tumor areas (Supplementary information, Figure S2A). Expression of B7-H3 was also detected on $CD45^-$ cells by immunofluorescence and was higher in the tumor than in the normal liver (Figure 1A). We also determined B7-H3 expression in human melanoma cells lines obtained from resected tumors. Although B7-H3 mRNA expression was found at different levels in the melanoma cell lines and DCs cultured *in vitro* (Figure 1B), B7-H3 protein was similarly highly expressed on these cells (Figure 1C). More importantly, protein expression of B7-H3 was found on macrophages and DCs derived from human melanoma infiltrates (Figure 1D). The B7-H3 receptor has not been identified [13] but previous results have indicated the presence of a putative receptor on activated T cells. To assess the expression of B7-H3 receptor in HCC patients, we tested the binding of a human B7-H3-mouse IgG2a fusion protein to lymphocytes in the peripheral blood mononuclear cells, normal liver, para-tumor, and tumor. We observed increased expression of B7-H3 receptor on $CD4^+$ and $CD8^+$ T cells in the liver compared to that in the peripheral blood (Supplementary information, Figure S2B). B7-H3 expression by tumor cells, tumor-infiltrating APCs, and B7-H3 receptor expression by lymphocytes strongly suggest their regulatory role in the tumor microenvironment.

To understand the functions of B7-H3 in murine tumors, we used an anti-B7-H3 antibody we previously generated [12], to examine B7-H3 expression. Surprisingly, we found B7-H3 intracellularly in both the mouse E.G7 lymphoma and B16-F10 melanoma cells but not on their surface (Figure 1E). The expression of B7-H3 mRNA was also found in these cells, ruling out the possibility of cross-reactivity in the intracellular staining

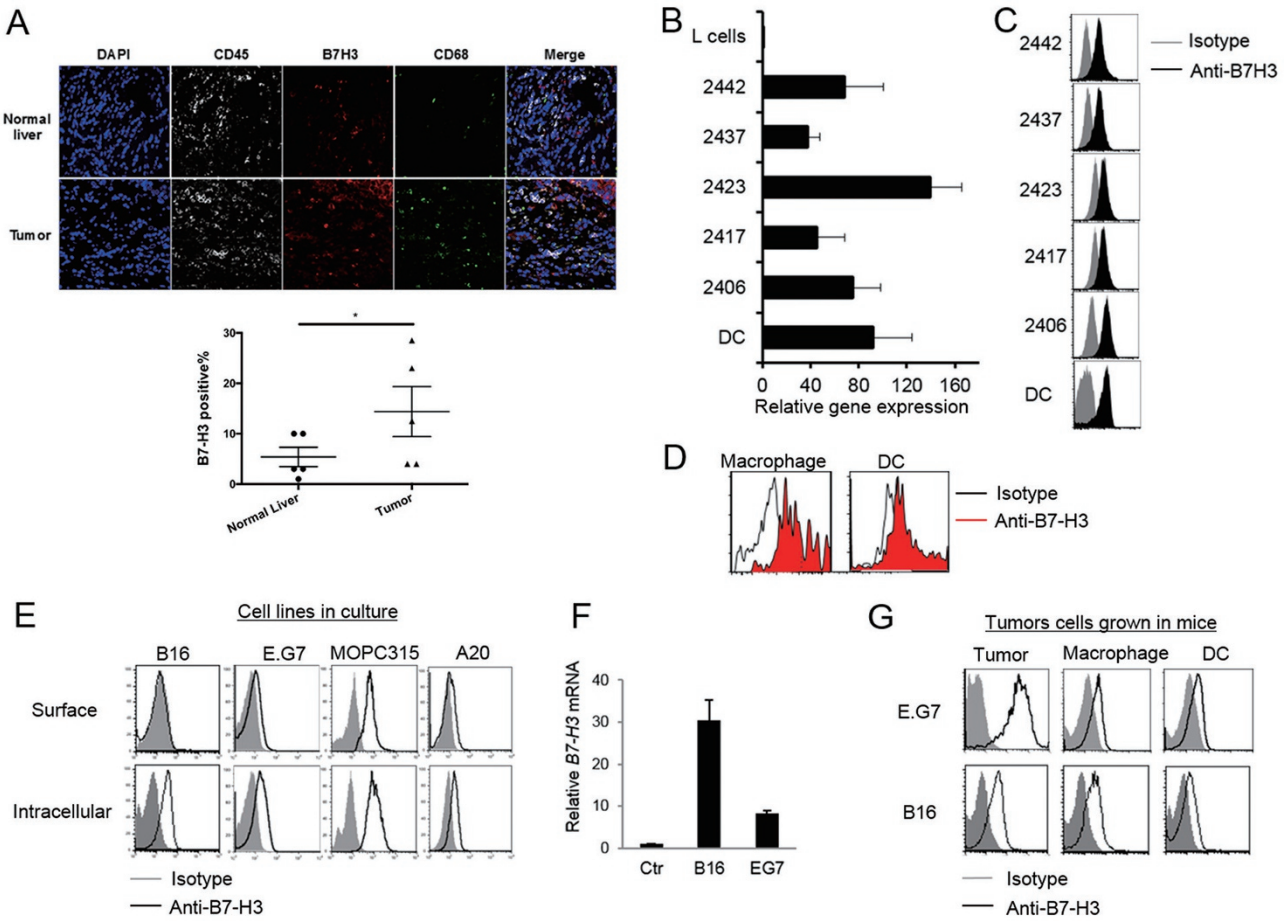

Figure 1 Expression of B7-H3 in human and murine tumors. **(A)** Representative images and summary histogram of immunofluorescence staining of B7-H3 together with DAPI, CD45 and CD68 in normal liver, paratumor, and tumor specimens from HCC patients. **(B)** mRNA levels of B7-H3 in melanoma cell lines derived from patients and *in vitro*-cultured DCs. **(C)** Protein expression of B7-H3 on the surface of human melanoma cell lines and *in vitro*-cultured DCs. **(D)** Expression of B7-H3 on the surface of tumor-infiltrating macrophages and DCs from melanoma patients. **(E)** Surface and intracellular expression of B7-H3 by B16, E.G7, MOPC315, and A20 in culture. **(F)** Transcripts of B7-H3 in B16 and E.G7. **(G)** Surface expression of B7-H3 on tumor cells, macrophage and DCs in the tumor of E.G7- and B16-bearing mice. **P* ≤ 0.05.

(Figure 1F). Interestingly, 7 days after inoculation in syngeneic mice, B7-H3 was highly expressed on the surface of both E.G7 and B16-F10 tumor cells (Figure 1G), suggesting its surface expression can be induced by the tumor microenvironment. MOPC 315 myeloma cells had both cell surface and intracellular B7-H3, whereas A20 lymphoma cells showed only its intracellular expression (Figure 1E). In addition to expression in the tumor cells, B7-H3 was also present on the surface of tumor-infiltrating macrophages and DCs in E.G7 and B16 models (Figure 1G). To investigate the expression of B7-H3 receptor on mouse tumor-infiltrating lymphocytes (TILs), we tested the binding of mouse B7-H3-Ig fusion protein to cells isolated from tumors and spleens of E.G7-bearing mice. Both NK and $CD8^+$ T cells from TILs and splenocytes (SPL) were strongly bound by mouse B7-H3-Ig protein. In contrast, $CD4^+$ T cells did not bind to B7-H3-Ig (Supplementary information, Figure S3A-S3B). Similar to E.G7 tumors, NK cells from B16-F10 melanoma also bound to B7-H3-Ig (Supplementary information, Figure S3C). These results suggest that B7-H3 might act on NK and $CD8^+$ T cells.

B7-H3 inhibition suppresses tumor development

To investigate the role of B7-H3 in tumor development, B7-H3-deficient (KO) [13] and wild-type (WT) mice, both on C57BL/6 background, were injected subcutaneously with E.G7 cells, and tumor growth was evaluated for 3 weeks. Lack of B7-H3 significantly reduced the growth of E.G7 cells to about 50% when compared

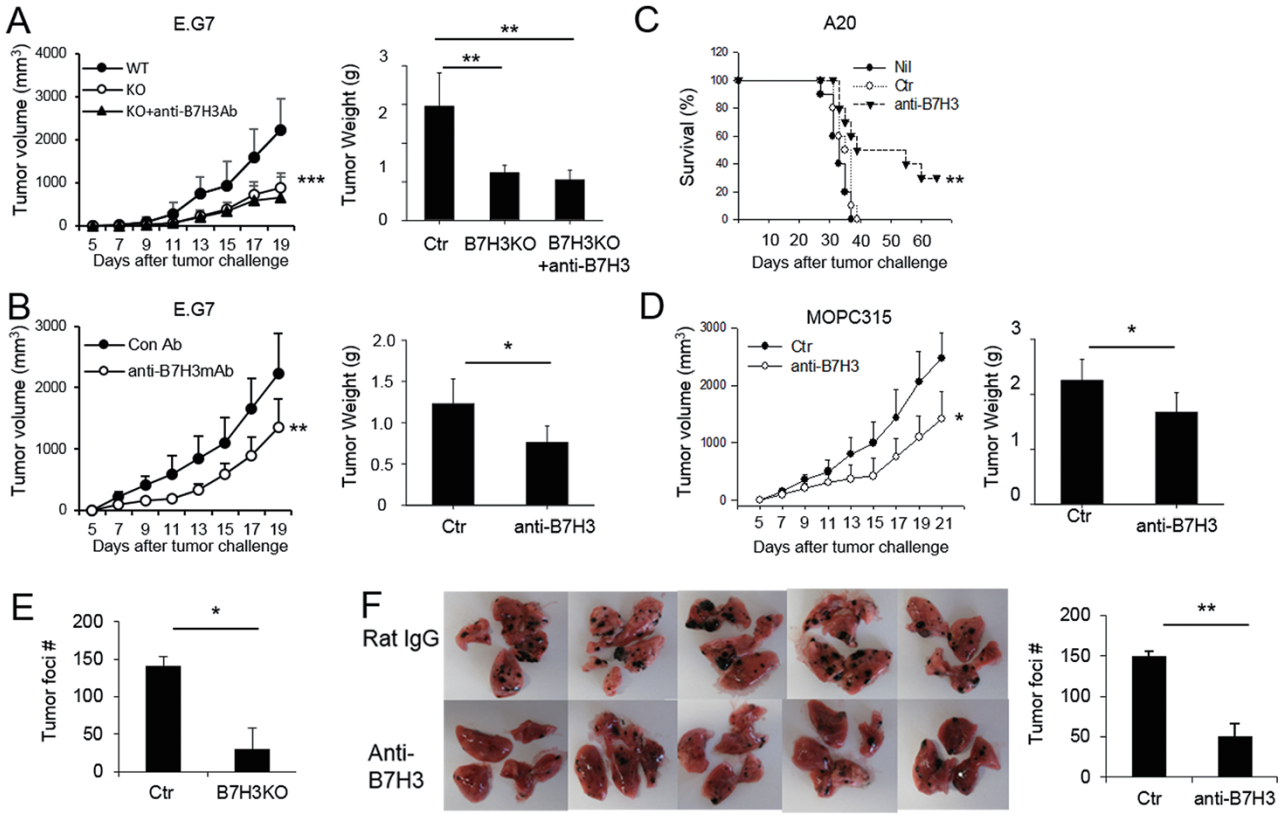

Figure 2 B7-H3 inhibition reduces tumor development in multiple cancer models. **(A)** Wild type (co-housed C57BL/6) mice (*n* = 5) or B7-H3 KO mice (*n* = 5) were challenged with 1 × 10^6 E.G7 cells administered sub-cutaneously. Tumor volume and tumor weight (Day 21) of wild type and B7-H3 KO mice are shown. C57BL/6 mice (*n* = 5) were challenged with 1 × 10^6 E.G7 or MOPC 315 cells. Balb/c mice (*n* = 4-5) were challenged with 1 × 10^6 A20. The Anti-B7-H3 Ab or control rat IgG was injected every other day for a period of 3 weeks. **(B)** Summary graphs showing tumor volume and tumor weight (Day 21) of E.G7-bearing mice treated with control Ab or anti-B7-H3. **(C)** Survival curves of A20-bearing mice treated with control Ab or anti-B7-H3 antibody are shown. **(D)** Summary data of tumor volume and tumor weight (Day 21) of MOPC315-bearing mice treated with control Ab or anti-B7-H3 antibody. **(E)** C57BL/6 mice (*n* = 5) or B7-H3 KO mice (*n* = 5) were challenged intravenously with 1 × 10^5 B16-F10 cells. On day 14, mice were euthanized for evaluation of tumor formation in their lungs. **(F)** C57BL/6 mice (*n* = 5) were challenged intravenously with 1 × 10^5 B16-F10 cells. Anti-B7-H3 or control rat was injected every 3 days for a period of 2 weeks. On day 14, mice were euthanized for evaluation of tumor formation in their lungs. Photographs show tumor foci in the lungs. A summary of the total numbers of foci per group of mice is also shown. Data are a representative of at least two separate experiments. *P* values were calculated with 2-way ANOVA or Kaplan-Meier methods by comparing control and B7-H3-deficient mice or mice treated with blocking Ab. **P* ≤ 0.05, ***P* ≤ 0.01.

to WT mice (Figure 2A). These data suggest that B7-H3 inhibition could enhance anti-tumor immunity. We therefore examined the therapeutic effects of B7-H3 blockade in multiple transplanted hematopoietic tumors using anti-B7-H3 blocking antibody. Syngeneic mice receiving live tumor cells on day 1 (intravenously for A20 and subcutaneously for E.G7 and MOPC315 cells) were treated with anti-B7-H3 antibody on day 3 followed by 10 injections every other day. Anti-B7-H3 treatment significantly reduced tumor growth in E.G7- or MOPC 315-bearing mice and prolonged the survival in > 30% of A20-bearing mice by at least 1 more month (Figure 2B-2D). Interestingly, anti-B7-H3-treated B7-H3 KO mice had similar tumor growth as the B7-H3 KO mice (Figure 2A), indicating that B7-H3 expression by host immune cells is more important and also suggesting that the antibody did not deplete tumor cells via antibody-dependent cellular cytotoxicity (ADCC).

Since B7-H3 expression was observed in human and murine melanoma, we also evaluated B16-F10 melanoma development in B7-H3 KO mice. The tumors cells were injected intravenously into the mice to promote melanoma colony growth in the lungs [18]. Fourteen days after the challenge, B7-H3 KO mice exhibited only 1/3 to 1/10

of the colonies found in WT mice (Figure 2E). Likewise, treatment with anti-B7-H3 blocking antibodies as a therapeutic regimen reduced B16-F10 growth in the lungs; the tumor foci formed in mice treated with anti-B7-H3 were smaller in size when compared to those treated with rat IgG (Figure 2F). Taken together, our results with hematopoietic and non-hematopoietic tumor models indicate the important role of B7-H3 in the development of multiple tumors from different tissue origins.

NK and CD8$^+$ T cells are required in B7-H3-mediated tumor immunity

To understand the functional mechanisms of B7-H3 in tumor development, we examined tumor-infiltrating immune cells as well as SPL from B7-H3 KO or WT mice harboring the E.G7 tumor. CD11b$^+$Gr1$^+$ cells, described as myeloid-derived suppressor cells [19], were reduced in the spleen and tumor of B7-H3 KO mice or mice treated with anti-B7-H3 when compared to the control groups (Supplementary information, Figure S4A-S4B). However, the population of regulatory T cells, also Ki-67 positive, did not show differences in the spleen and tumors of B7-H3 KO and WT mice, respectively (Supplementary information, Figure S4C-S4D).

To determine the functional target cell of B7-H3 in our tumor models, CD4$^+$, CD8$^+$, or NK cells were depleted using selective mAbs before challenging with the E.G7 tumor. Interestingly, depletion of NK cells or CD8$^+$ T cells greatly prevented the control of tumor growth seen in B7-H3 KO mice. Double depletion of NK and CD8$^+$ T cells further abrogated the suppression of tumor growth in B7-H3 KO mice. In contrast, depletion of CD4$^+$ T cells did not influence the tumor growth in B7-H3 KO mice (Figure 3A-3B). We also confirmed that depletion of NK cells or CD8$^+$ T cells reduced the anti-tumor effect of anti-B7-H3 Ab treatment (Supplementary information, Figure S5A). Moreover, mice depleted of both CD8$^+$ T and NK cells developed larger tumors than mice with single depletion. Similarly, in the B16-F10 melanoma model, depletion of NK cells in B7-H3 KO mice increased the numbers of tumor foci (Figure 3C). However, depletion of CD8$^+$ T cells did not have any effect on lung

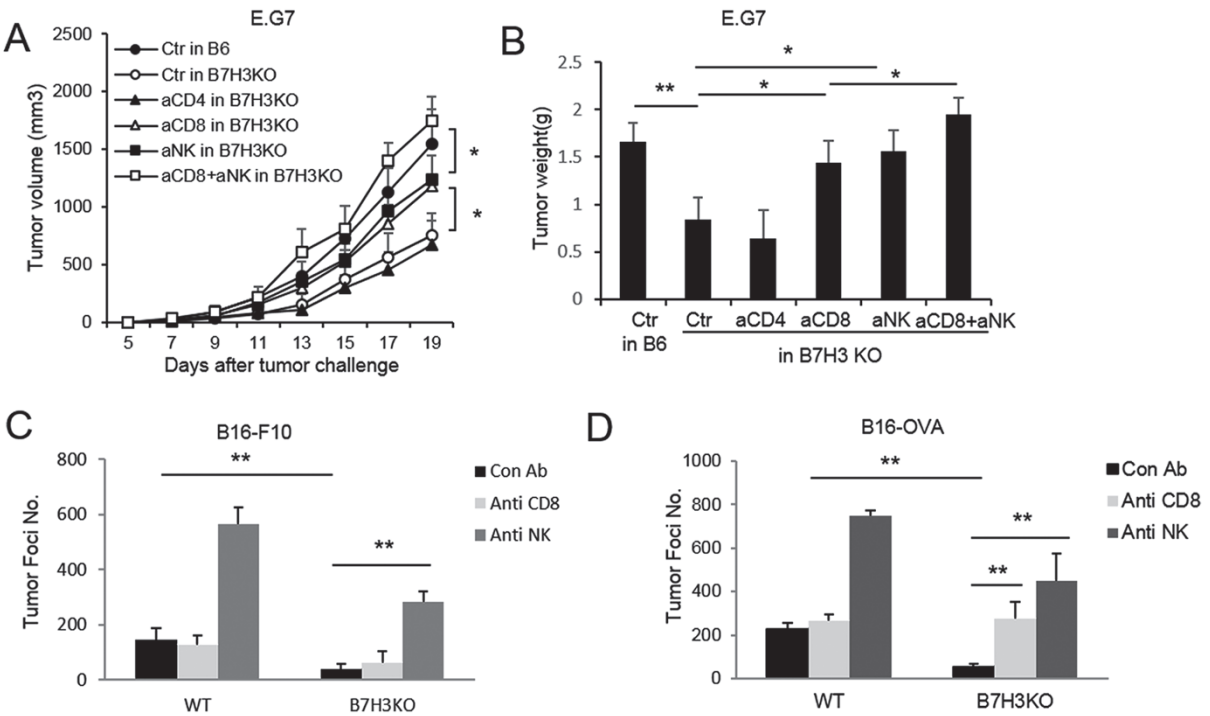

Figure 3 Anti-tumor effect by B7-H3 inhibition is dependent on CD8$^+$ T and NK cells. C57BL/6 mice (n = 3-5) or B7-H3 KO mice (n = 3-5) were challenged with 1 × 10^6 E.G7 cells and anti-CD4 (GK1.5 mAb), anti-CD8 (53.6.7 mAb), anti-NK (ASGM1 mAb), or control Ab was injected intravenously 1 and 3 days before the tumor challenge. Tumor volume was measured every other day. On day 21, mice were euthanized and tumors were weighed. Growth **(A)** and weight **(B)** of E.G7 tumor on WT or B7-H3 KO mice with or without depletion of CD8$^+$ T, CD4$^+$ T, or NK cells are shown. **(C)** Summary of total number of tumor foci in the lung in WT and B7-H3 KO mice challenged with B16-F10 with or without depletion of CD8$^+$ T or NK cells. **(D)** Summary of total numbers of tumor foci in the lung of wild type and B7-H3 KO mice challenged with B16-OVA with or without depletion of CD8$^+$ T or NK cells. Data are a representative of at least two separate experiments. *$P \le 0.05$, **$P \le 0.01$.

metastasis in B7-H3 KO mice, consistent with the poor ability of B16-F10 to induce $CD8^+$ T cell responses [20]. Interestingly, when the B16-OVA line was used, $CD8^+$ T cells became important in B7-H3 inhibition-mediated tumor reduction (Figure 3D). Taken together, these results indicate that anti-tumor immunity generated by B7-H3 inhibition is dependent on $CD8^+$ T cells and especially NK cells.

B7-H3 regulates anti-tumor $CD8^+$ T cells

When TILs were phenotypically evaluated, the proportions of $CD4^+$ and $CD8^+$ T cells did not change in the tumor of B7-H3 KO mice (Figure 4A). Since E.G7 tumors express ovalbumin (OVA) antigen, we evaluated OVA-reactive $CD8^+$ T cells from TILs. SIINFEKL tetramer positive cells were doubled in tumors from B7-H3 KO mice compared to WT mice (Figure 4B). Further analysis revealed that these $CD8^+$ T cells expressed increased levels of IFN-γ and Granzyme B. Percentage of IFN-γ^+ and Granzyme B^+ $CD4^+$ TILs was also increased in B7-H3-deficient mice (Figure 4C). Interestingly, depletion of NK cells substantially reduced Granzyme B-expressing $CD8^+$ T cells in the TILs, while depletion of $CD8^+$ T cells reduced expression of Granzyme B by tumor-infiltrating NK cells in B7-H3-deficient mice (Figure 4D). Also, $CD8^+$ T cells and NK cells in the tumor

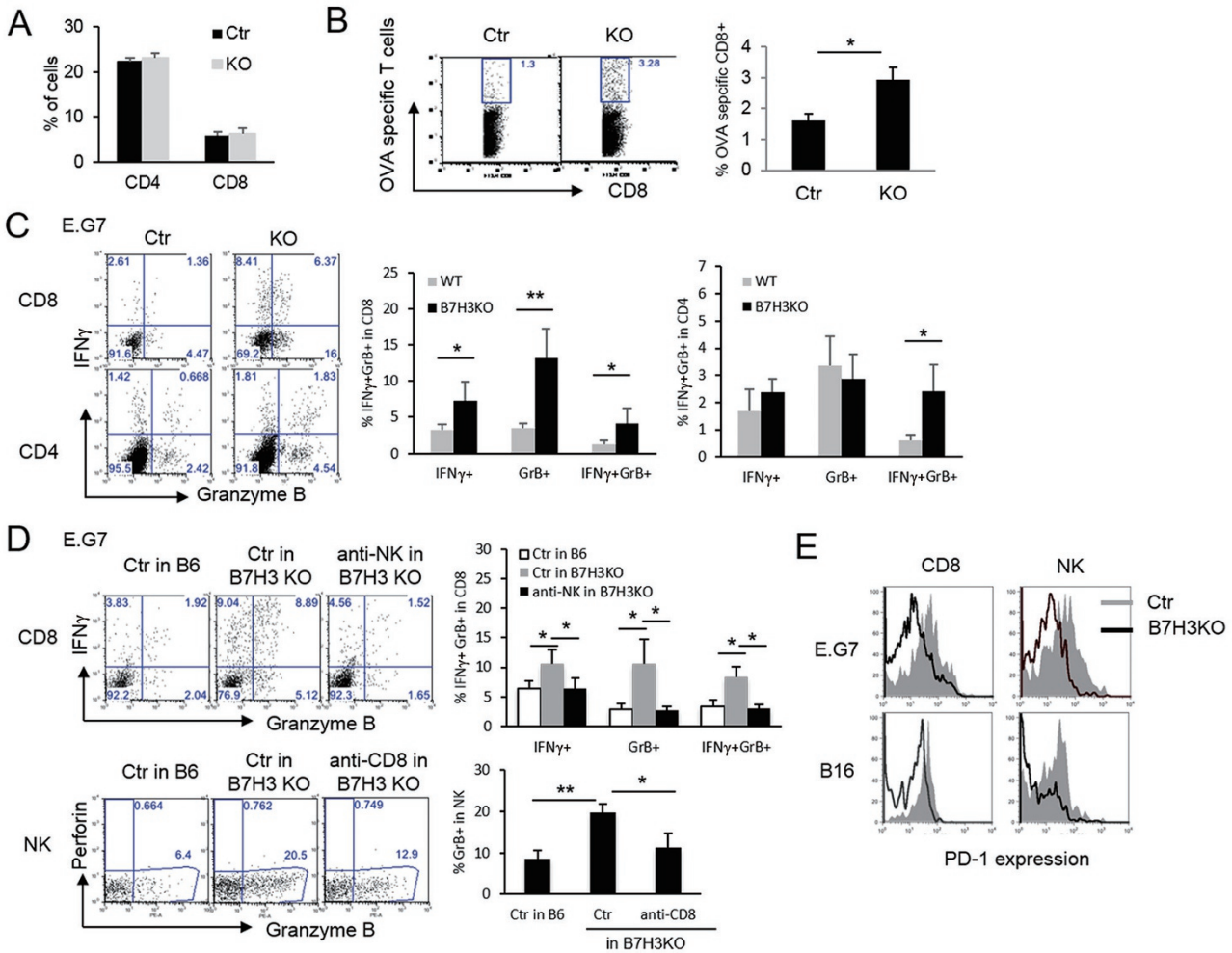

Figure 4 B7-H3 regulates tumor-infiltrating $CD8^+$ T cells. **(A)** Percentage of $CD4^+$ and $CD8^+$ T cells in the TIL of wild type and B7-H3 KO mice. **(B)** Representative plots and summary histogram showing frequency of OVA-specific $CD8^+$ T cells in total $CD8^+$ T cells in the tumor of E.G7-bearing WT and B7-H3 KO mice. **(C)** Intracellular staining of IFN-γ and Granzyme B in tumor-infiltrating $CD8^+$ and $CD4^+$ T cells from E.G7-bearing WT and B7-H3 KO mice after re-stimulation by PMA/ionomycin. **(D)** Intracellular staining of IFN-γ and Granzyme B in $CD8^+$ and NK TIL from E.G7-bearing WT and B7-H3 KO mice treated with control, NK-depleting, or CD8-depleting antibodies. **(E)** Expression of PD-1 on $CD8^+$ T and NK cells in the tumor of E.G7- or B16-bearing WT and B7-H3 KO mice. $^*P \le 0.05$, $^{**}P \le 0.01$.

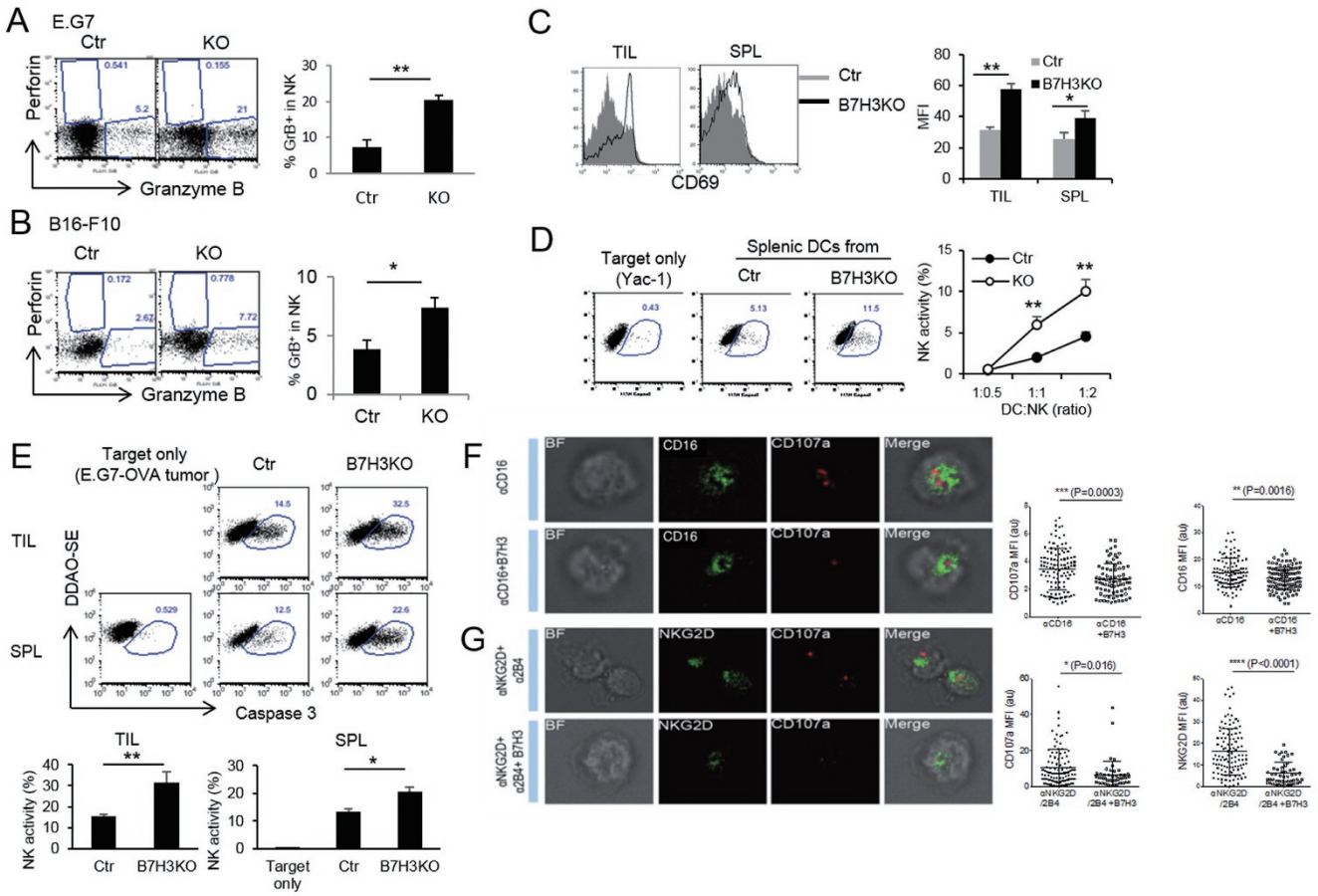

Figure 5 B7-H3 inhibition increases NK-cell function. **(A)** Expression of Perforin and Granzyme B by NK cells from E.G7-bearing WT and B7-H3 KO mice after re-stimulation. **(B)** Expression of Perforin and Granzyme B by NK cells from B16-F10-bearing WT and B7-H3 KO mice after re-stimulation. **(C)** CD69 expression by NK (NK1.1+DX5+CD3-) cells from WT or B7-H3 KO mice bearing the E.G7 tumor. **(D)** Killing capacity of NK cells pre-activated by LPS-stimulated wild-type or B7-H3 KO DCs. **(E)** *Ex vivo* cytolytic function of NK cells from the spleen and tumor of E.G7-bearing WT and B7-H3 KO mice. **(F-G)** Quantification of CD107a mean fluorescence intensity on the plasma membrane of freshly isolated human NK cells. Primary NK cells were activated on bilayers carrying anti-CD16-Alexa Fluor 488 (green, **F**) or anti-NKG2D Alexa Fluor 488 in the presence of unlabeled anti-2B4 (green, **G**). Data pooled from two independent experiments. **P* ≤ 0.05, ***P* ≤ 0.01, ****P* ≤ 0.001.

tissues of B7-H3 KO mice had reduced PD-1 expression when compared to cells in WT mice (Figure 4E). We also tested whether B7-H3 inhibits $CD8^+$ T-cell activation in *in vitro* co-culture of DCs and $CD8^+$ T cells. Splenic DCs from WT or B7-H3 KO mice were isolated and co-cultured with CFSE-labeled OVA-specific $CD8^+$ T cells (OT-I) *in vitro* for 3 days and proliferation was evaluated by dilution of CFSE intensity. DCs from B7-H3 KO mice induced increased proliferation of OT-I T cells compared with DCs from WT mice (Supplementary information, Figure S4E). More importantly, OT-I T cells stimulated by DCs from B7-H3 KO mice displayed remarkably higher expression of Granzyme B and IFN-γ compared with those stimulated by DCs from WT mice (Supplementary information, Figure S4E). Thus, B7-H3 inhibition might enhance the number and cytolytic function of tumor antigen-specific $CD8^+$ T cells.

B7-H3 regulates NK-cell function

To understand the role of B7-H3 in regulating NK-cell-mediated tumor protection, we analyzed the quantity and function of NK cells in E.G7- or B16.F10-tumors developing in WT or B7-H3-deficient host mice. The percentage and absolute number of NK cells were increased in the B7-H3 KO mice (Supplementary information, Figure S5B-S5C). Furthermore, B7-H3 KO mice showed a substantial increase in Granzyme B-producing NK cells in TILs from both E.G7- and B16.F10-bearing mice (Figure 5A-5B). CD69, an NK activation marker, was upregulated on NK cells in the spleen and tumors from

B7-H3 KO mice (Figure 5C and Supplementary information, Figure S5D). To determine regulation of the NK killing function by B7-H3, NK cells were isolated from spleen and TILs of E.G7-bearing mice and the killing of E.G7 cells tested *in vitro* by detection of cleaved levels of caspase-3 [21]. NK cells from B7-H3 KO mice were more efficient in tumor killing when compared with those from control mice (two-fold increase) (Figure 5E). These results indicate that B7-H3 controls NK-cell activation in the tumor microenvironment. Since B7-H3 is expressed by DCs, we tested whether DCs derived from B7-H3 KO mice could induce NK-cell activation more effectively *in vitro*. DCs isolated from WT or B7-H3 KO mice were stimulated with LPS for 18 h before being co-cultured with NK cells. After overnight activation with the DCs, killing of YAC-1 cells by NK cells was evaluated using the Caspase3-based assay. DCs from B7-H3 KO mice induced a stronger NK-mediated killing activity than WT DCs (Figure 5D) thus supporting a role for B7-H3 in inhibition of NK-cell activation.

To investigate the potential effect of the B7-H3 molecule on human NK cells, their degranulation was tested in an *in vitro* ADCC assay. Briefly, the fluorescence intensity of the CD107a molecule on the plasma membrane of NK cells (a marker for NK-cell degranulation) was assessed by confocal microscopy of NK cells placed on lipid bilayers coated with antibodies against CD16 to mediate ADCC, in the presence or absence of B7-H3-Ig. When NK cells were incubated on bilayers carrying anti-CD16 alone, a strong CD107a signal accumulated at the center of the synapse, which was indicated by the central clustering of anti-CD16 molecules on the lipid bilayer (Figure 5F). However, when NK cells were incubated on bilayer containing anti-CD16 in combination with B7-H3-Ig, the mean fluorescence intensity of CD107a on the PM of NK cells was decreased (Figure 5F). Further analysis of CD16 clusters on the lipid bilayer revealed that B7-H3-Ig significantly decreased the accumulation of anti-CD16 molecules on the lipid bilayer (Figure 5F). Similar results were observed on a lipid bilayer containing NKG2D and 2B4 antibodies to induce natural cytotoxicity, with and without B7-H3 (Figure 5G). NK cells placed on control lipid bilayers loaded with IgG in the presence or absence of B7-H3 had no detectable CD107a fluorescence (Supplementary information, Figure S6).

Combination therapy with anti-B7-H3 and anti-PD-1

Based on our data, it seemed that B7-H3 should be a good target for immunotherapy against lymphoma and melanoma because blocking of B7-H3 with a specific antibody induced anti-tumor immunity. Since B7-H3 and PD-L1 were expressed in the E.G7 model and in human cancers, we decided to test the blockade of B7-H3 in the context of a PD-1 blockade, which has already shown significant anti-tumor effects in human cancers [6, 22]. Groups of C57BL/6 mice were subcutaneously transplanted with 1×10^6 E.G7 cells and treated with intraperitoneal injection of control, anti-B7-H3 antibody, anti-PD-1 antibody, or anti-B7-H3 plus anti-PD-1 antibodies one day 7, 10, 13, 16, and 19, respectively. Although treatment with a single antibody against B7-H3 or PD-1 exhibited an anti-tumor effect, the combined anti-B7-H3 and anti-PD-1 antibody treatment further reduced tumor volume and tumor weight (Figure 6A). In contrast, earlier treatment with a combinational blockade starting from day 3 did not show synergistic effects, as the single antibody treatment was already effective (Figure 6B). Therefore, combination therapy with anti-B7-H3 and anti-PD-1 can generate powerful anti-tumor immunity, especially in late-stage cancers.

Discussion

Immunotherapy has arisen as a new type of treatment for cancer. Considerable success has been achieved in multiple cancers, including melanoma, by use of checkpoint inhibitors anti-CTLA4 and/or anti-PD-1/PD-L1 [4, 6]. These exciting advancements in the clinic have implicated other co-inhibitory molecules as potential targets for cancers. Here, we report the function of B7-H3 in several transplantation tumor models, highlighting this molecule as a potential target for cancer immunotherapy.

Although B7-H3 was originally described as a positive regulator of T cells in humans [10], growing evidence has indicted that it may indeed be a negative regulator. Lack or inhibition of B7-H3 resulted in enhanced autoimmunity [12, 13]. Recently, it was also found that B7-H3 also potently inhibited human T-cell activation [14]. In this paper, we showed that both murine and human B7-H3 inhibited NK-cell activation. The reason underlying the different results is unclear, in part because the receptor for B7-H3 has not been identified. Although it has been suggested that TLT2 is a receptor for B7-H3 [23], it has not been confirmed by others and us in another study [14]. Thus, it will be important in the near future to identify the B7-H3 receptor in order to fully determine the diverse functions of B7-H3, and also to detail the inhibitory signaling pathway. The variable function of B7-H3 may be caused by differential glycosylation, which has been reported in B7-H3 molecules expressed in oral squamous cell carcinoma [24]. This suggests that glycosylation of B7-H3 in tumors regulates B7-H3's immune function. The anti-B7-H3 blockade may be happening on APCs infiltrating the tumor cells. So far it is unknown

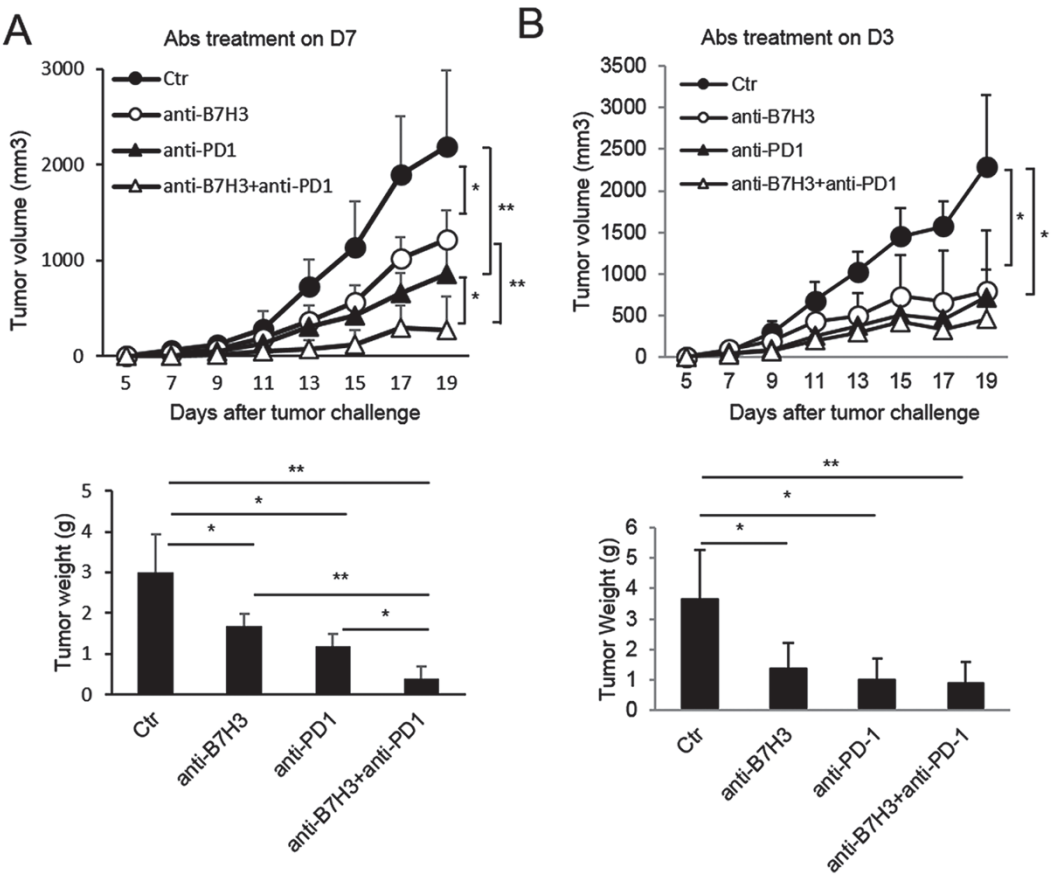

Figure 6 Enhanced protective effect by B7-H3 and PD-1 dual blockade. (**A**-**B**) Groups of C57BL/6 mice were s.c. transplanted with 1 x 10^6 E.G7 cells and given an intra-peritoneal injection of control IgG, anti-B7-H3 (100 μg), anti-PD-1 (100 μg), or anti-B7-H3 plus anti-PD-1 antibody starting on day 3 **(B)** or 7 **(A)** and every 3 days for a period of 3 weeks . Tumor volume was measured every other day. Data are a representative of at least two separate experiments. *$P \leq 0.05$, **$P \leq 0.01$.

whether B7-H3 functions via the infiltrating DC, macrophages, and/or the tumor cells. In the E.G7 model at least, the function of B7-H3 appears to be most important in the non-tumor cells, most likely the tumor-infiltrating DCs and macrophages. Indeed, we found that DCs lacking B7-H3 are more potent in the induction of NK and $CD8^+$ T-cell function. However, it is likely that in another context, tumor expression of B7-H3 may also be important. Our anti-B7-H3 did not have depletion effect on DCs and macrophages, suggesting that it modulates immune cell function instead.

B7-H3 expression has been associated with poor prognosis in multiple cancers [16, 17, 25-28]. In this study, we found that lack of B7-H3 suppressed the development of multiple cancers. Moreover, anti-B7-H3 had potent therapeutic effects in multiple murine models. Interestingly, we found that the function of B7-H3 was dependent on NK cells and $CD8^+$ T cells. Although B7-H3 also negatively regulated $CD8^+$ T-cell activation, B7-H3 function in the B16-F10 model was primarily mediated by NK cells indicating that B7-H3 function may vary depending on the tumor origins. B7-H3 inhibits both mouse and human NK-cell activation, in accord with previous reports which described B7-H3 binding to NK cells [29]. However, although both WT and KO groups of mice treated with anti-NK antibody had more tumor colonies than mice treated with control antibody, the NK-depleted KO mice did not develop as many colonies as the WT mice treated with anti-NK antibodies. We suggest this could be due to incomplete depletion of NK cells, or because of compensation by $CD8^+$ T cells. Indeed, double depletion of NK and $CD8^+$ T cells resulted in even greater tumor growth (Figure 3). In contrast to the B7-H3 receptor, PD-1 is not highly expressed by NK cells and previously we did not find a therapeutic effect of anti-PD-L1 in the B16-F10 model [9]. This suggests a separation of labor such that B7-H3 co-inhibits NK cells while PD-1 primarily acts on $CD8^+$ T cells. This may

underscore the synergistic effects of B7-H3 and PD-1 antibodies in late stage cancer.

Overall, our data strongly support for a role of B7-H3 in tumor immunity and suggest the potential value of targeting the B7-H3 checkpoint alone or together with PD-1 to serve as a new immunotherapy against cancers.

Materials and Methods

Patients and specimens

Fresh specimens and matched blood of HCC patients were obtained from the China-Japan Friendship Hospital. For isolation of tissue-infiltrating leukocytes, fresh normal liver, paratumor, and tumor specimens from HCC patients were digested in RPMI-1640 medium supplemented with 0.5 mg/ml Collagenase Type IV (Gibco), 10% FBS plus 10 U/ml DNase I, minced into small pieces manually, and then transferred to 70 μm cell strainers (BD) and mechanically separated using the plunger of a 5-ml syringe. The cells passing through the cell strainer were collected and subjected to Ficoll-Hypaque gradient centrifugation. After centrifugation, mononuclear cells were recovered and stored at −80 ºC until flow cytometry analysis or immediately used for experiments. For immunofluorescence staining, all samples were fixed in formalin solution and embedded in paraffin. Sections were dewaxed in xylene, dehydrated in ethanol, and incubated in 3% H_2O_2 for 15 min to destroy the activity of endogenous peroxidase. After blocking with 10% normal donkey serum, each slide was incubated with the primary antibodies at 4 ºC overnight. AffiniPure F(ab′)$_2$ Fragment donkey anti-rabbit/mouse/goat immunoglobulin was chosen as the second antibody. All experimental protocols were approved by the institutional review committee.

Expression and purification of human B7-H3-mIgG2a Fc fusion protein

Using an expression vector pcDNA3.4 (ThermoFisher Scientific), human B7-H3-mIgG2a Fc fusion protein, which contains amino acids Leu29-Pro245 of the B7-H3 extracellular domain (NCBI: NP_079516) and amino acids Pro99-Lys330 of the mouse IgG2a Fc fragment (GeBank: CAA24178.1), was transfected into FreeStyle 293-F cells (ThermoFisher Scientific). Cell culture supernatants were collected at 96h post-transfection. A protein A affinity column was pre-equilibrated with 20 mM Na_2HPO_4 buffer with 0.15 M NaCl, pH 7.2. Bound B7-H3-mIgG2a fusion protein was eluted with 0.1 M Glycine (pH 2.7), and dialyzed in PBS buffer (pH 7.2).

Evaluation of B7-H3 expression

Melanoma cell lines, 2406, 2417, 2423, 2437, and 2442 were derived from melanoma tissue resected during surgery using clinical and laboratory protocols approved by the MD Anderson Cancer Center Institutional Review Board. Cell lines were grown and mRNA isolation was performed as previously reported [18]. RT-PCR was done using a Cyber green based kit (Bio-Rad, CA, USA) with the following primers: Forward 5′-AGCACTGTGGTTCTGCC TCACA -3′ Reverse 5′-CACCAGCTGTTTGGTATCTGTCAG-3′. Surface expression of B7-H3 was evaluated using 110 mAb reported previously [12] followed by a biotinylated anti-Rat antibody and streptavidin Alexafluor 488 (Life Technologies, CA, USA). For the B7-H3-Ig binding assay, $CD4^+$, $CD8^+$, and NK cells were isolated from TILs or SPL of E.G7-bearing mice, and the B7-H3-Ig-binding assay determined as previously reported [11].

Mice

C57BL/6 and Balb/c mice were purchased from the Jackson Laboratory or NCI facility. B7-H3- deficient mice (C57BL/6 background) or co-housing B6 mice were bred at MD Anderson SPF facility. Mice were used at 6-10 weeks of age. The animal protocol (05-05-04233) was approved by the IACUC of MD Anderson.

Tumor experiments

C57BL/6 mice or B7-H3 KO mice of the same background were injected intravenously with 1×10^5 B16-F10 cells to promote melanoma growth in the lung, and 2 weeks later the mice were euthanized to evaluate tumor foci numbers in the lungs. Skin lymphomas were grown in C57BL/6 or B7-H3 KO mice by injecting 1×10^6 E.G7 cells sub-cutaneously, and tumor size was monitored using a caliper. Similarly, Balb/c mice were intravenously injected with 1×10^6 A20 lymphoma or subcutaneously with 1×10^6 MOPC 315 myeloma cells. Survival was evaluated in mice injected with A20 and tumor growth in MOPC 315 injected mice. Mice were sacrificed when the tumor diameters reached 20 mm. B7-H3 blockade was performed by injecting intraperitoneally 100 μg of anti-B7-H3 mAb (clone 110) or control rat IgG on the indicated days. A20- and MOPC 315-bearing mice received a total of 10 injections of antibodies and B16-F10-bearing mice 5 injections. Survival was monitored for 70 days after tumor challenge. Tumor volume was calculated by the ellipse formula, length/2 × width/2 × π. Blocking antibodies for B7-H3 (clone 110) and PD-1 (clone J43) were produced in high quantities by BioXcell (NH, USA).

Antibody-mediated depletion

Monoclonal anti-CD4 (GK1.5) and anti-CD8 (523.7) antibodies (Abs) were purchased from BioXcell (NH, USA) and NK depletion Ab—asialo-GM1 (ASGM1) from WAKO Pure Chemicals (Osaka, Japan). To deplete CD4, CD8, or NK cells, 100 μg of anti-CD4 or anti-CD8 mAb, or 50 μg ASGM1 antibodies were injected intraperitoneally twice (on days 3 and 1) into the mice. On day 0, mice were challenged with 1×10^6 live E.G7 (subcutaneously injected), 1×10^5 B16.F10 cells (intravenously injected), or 1×10^5 B16.OVA (intravenous injection).

Isolation of tumor-infiltrating cells

Tumor-infiltrating cells from lungs were isolated using a previously described protocol [18]. Briefly, tumors were digested with 1 mg/ml collagenase D for 1 h at 37 °C, and the lymphocyte faction was isolated after gradient-centrifugation of the cell suspension. Lymphocyte fractions were counted and used for flow cytometry analysis.

Antibodies and flow cytometry

The following fluorescent dye-conjugated anti-human antibodies were used for staining: anti-CD45 (HI30), anti-HLA-DR (L243), anti-CD11c (3.9), anti-B7-H3 (DCN.70), Streptavidin-BV421, anti-CD3 (OKT3), and anti-CD56 (HCD56) (Biolegend, CA, USA); anti-CD14 (MP9), anti-CD123 (7G3), and anti-CD8 (SK1) (BD biosciences, CA, USA). Antibodies to mouse proteins were as follows: anti-CD4 (GK1.5), anti-CD8 (53-6.7), anti-CD11b (M1/70), anti-CD69 (H1.2F3), anti-PD-1 (J43), anti-Gr1 (1A8), anti-NK1.1

(PK136), anti-IFN-γ (XMG1.2), and anti-Caspase3 (C92-605) were all purchased from BD biosciences. Antibodies against CD16 (3G8), Granzyme B (GB11) were purchased from Biolegend. Anti-perforin (eBioOMAK-D), anti-ki67 (SolA15), and biotinylated anti-2B4 (ebioC1.7) antibodies were purchase from e-bioscience (MA, USA). Anti-NKG2D (MAB139) and recombinant His-tag B7-H3 protein were purchased from R&D System (MN, USA). Mouse IgG1 (MOPC21) was purchased from Sigma-Aldrich (MO, USA). Anti-CD107a (clone H4A3) was purchased from Developmental Studies Hybridoma Bank in University of Iowa (IA, USA). The 1,2-Dioleoyl-sn-Glycero-3-Phosphocholine (DOPC), 18:1 Biotinyl Cap PE 1,2-dioleoyl-sn-glycero-3-phosphoethanolamine-N-(cap biotinyl) and 1,2-Dioleoyl-sn-Glycero-3-[(N-(5-amino-1-carboxypentyl) iminodiacetic acid) succinyl] (Nickel salt) (DOGS-NTA) were from Avanti Polar Lipids Inc (AL, USA). PE-H2-K^b pentamer carrying the OVA257–264 peptide (SIINFEKL) was purchased from Proimmune (FL, USA). Surface immunofluorescence staining was performed at 4 °C for 20 min. Cytokine intracellular staining was performed after re-stimulation with PMA/ionomycin in the presence of Golgi-Plug for 5 h. For the pentamer staining, cells were stained with CD8 and further stained with PE-H2-K^b pentamer at room temperature for 1 h. Samples were analyzed in a FACScalibur equipped with DIVA software respectively. Files were analyzed using FlowJo.

Murine NK-cell functional assay

The *ex vivo* NK killing activity was measured using a Caspase-3 cleavage assay [21]. In brief, NK cells were isolated from spleen or TILs in E.G7 bearing B7-H3 KO or WT mice by sorting CD3-NK1.1+ with a FACS Aria. E.G7 tumor cells were used as target cells after labeled with DDAO-SE. The sorted NK cells were co-cultured with DDAO-SE-labeled target E.G7 cells at a 1:1 ratio for 3 h at 37 °C. The cells were permeabilized and stained with PE-conjugated anti-cleaved Caspase-3 antibody. The percentages of cleaved Caspase-3-positive cells among DDAO-SE-labeled target cells were analyzed by flow cytometry.

To test APC-mediated NK activity, splenic DCs were isolated from WT or B7-H3 KO mice and stimulated with LPS (100 ng/ml) and NK cells overnight at 37 °C. DDAO-SE-labeled target YAC-1 cells were co-cultured for 3 h and NK killing activity was analyzed by determining the proportions of caspase-3 staining YAC-1 cells.

Human NK (CD107a) functional assay on planar lipid bilayer

Human NK cells were isolated from peripheral blood using the NK-cell isolation kit (Miltenyi) according to the manufacture's instructions. Resting NK cells ($CD3^-$ $CD56^+$) of > 95% purity were suspended in IMDM as described previously [30].

The preparation of a planar lipid bilayer was described previously [30, 31]. CD107a F(ab′)2 antibody was prepared using the F(ab′)2 preparation kit (Pierce), and then labeled with Alexa Fluor 647 (Life Technologies). Mouse IgG1, anti-CD16 antibody, and anti-NKG2D were biotinylated using EZ-Link NHS-PEG4 Biotinylation Kit (Pierce, MA, USA) and further labeled with Alexa Fluor 568 (Life Technologies). All Dye-conjugated antibodies were further purified by Sepharyl S-200 size exclusion HPLC. The freshly isolated NK cells mixed with Alexa Fluor 647-labeled CD107a F(ab′)2 antibody, were injected into the lipid bilayers containing 0.5 μg/ml anti-CD16 antibody, or 0.25 μg/ml anti-NKG2D plus 0.25 μg/ml anti-2B4 with or without 1 μg/ml B7-H3 protein for 1 h at 37 °C. Cells were then fixed with freshly preparation 4% paraformaldehyde. Confocal images were acquired on a Leica gated stimulated emission depletion microscopy using a 100 × 1.4 objective. The lipid bilayer panel was determined by the maximal intensity of Alexa Fluor 568 signal. Image analysis was carried on using Volocity (PerkinElmer, MA, USA) or LAS AF (Leica, Wetzlar, Germany).

Statistical analysis

Statistical comparisons were performed using a two-tail paired Student's *t*-test as indicated. $P < 0.05$ were considered statistically significant. The correlation of tumor volume was analyzed for significance using two-way analysis of variance (ANOVA). The Kaplan-Meier method was used to estimate the survival outcomes and groups were compared with log-rank statistic.

Acknowledgments

This work was supported by grants from Beijing Municipal Science and Technology (Z171100000417005 to CD) and supported in part by grant from the National Natural Science Foundation of China (81502462 to LN). CD is a Bayer Chair Professor of Tsinghua University.

Author Contributions

YHL and NMO performed most of the experiments; PZ, JL, PZ, HT, HJP, MJ, SHC, BSK, WX, WZ, LG, YL, ZJD, WWO, PH, QY, LK, ZY, TWM, WL, LGR, LN and DL performed some of the experiments or contributed to their design; YHL and CD wrote the manuscript; CD supervised the study.

Competing Financial Interests

NMO and LGR are employees of EMD Serono Research and Development Institute. LG is an employee of X-KANG United Biopharmaceutical Science & Technology Co. Ltd.

References

1 Sharpe AH, Freeman GJ. The B7-CD28 superfamily. *Nat Rev Immunol* 2002; **2**:116-126.
2 Nurieva RI, Liu X, Dong C. Yin–Yang of costimulation: crucial controls of immune tolerance and function. *Immunol Rev* 2009; **229**:88-100.
3 Martin-Orozco N, Dong C. Inhibitory costimulation and anti-tumor immunity. *Semin Cancer Biol* 2007; **17**:288-298.
4 Curiel TJ, Wei S, Dong H, *et al.* Blockade of B7-H1 improves myeloid dendritic cell-mediated antitumor immunity. *Nat Med* 2003; **9**:562-567.
5 Fong L, Small EJ. Anti-cytotoxic T-lymphocyte antigen-4 antibody: the first in an emerging class of immunomodulatory antibodies for cancer treatment. *J Clin Oncol* 2008; **26**:5275-5283.
6 McDermott DF, Atkins MB. PD-1 as a potential target in cancer therapy. *Cancer Med* 2013; **2**:662-673.
7 Topalian SL, Hodi FS, Brahmer JR, *et al.* Safety, activity, and immune correlates of anti-PD-1 antibody in cancer. *New Engl J Med* 2012; **366**:2443-2454.

8 Boorjian SA, Sheinin Y, Crispen PL, *et al.* T-cell coregulatory molecule expression in urothelial cell carcinoma: clinicopathologic correlations and association with survival. *Clin Cancer Res* 2008; **14**:4800-4808.
9 Singh M, Khong H, Dai Z, *et al.* Effective innate and adaptive antimelanoma immunity through localized TLR7/8 activation. *J Immunol* 2014; **193**:4722-4731.
10 Chapoval AI, Ni J, Lau JS, *et al.* B7-H3: a costimulatory molecule for T cell activation and IFN-gamma production. *Nat Immunol* 2001; **2**:269-274.
11 Sun M, Richards S, Prasad DV, Mai XM, Rudensky A, Dong C. Characterization of mouse and human B7-H3 genes. *J Immunol* 2002; **168**:6294-6297.
12 Prasad DV, Nguyen T, Li Z, *et al.* Murine B7-H3 is a negative regulator of T cells. *J Immunol* 2004; **173**:2500-2506.
13 Suh WK, Gajewska BU, Okada H, *et al.* The B7 family member B7-H3 preferentially down-regulates T helper type 1-mediated immune responses. *Nat Immunol* 2003; **4**:899-906.
14 Leitner J, Klauser C, Pickl WF, *et al.* B7-H3 is a potent inhibitor of human T-cell activation: no evidence for B7-H3 and TREML2 interaction. *Eur J Immunol* 2009; **39**:1754-1764.
15 Sun J, Chen LJ, Zhang GB, *et al.* Clinical significance and regulation of the costimulatory molecule B7-H3 in human colorectal carcinoma. *Cancer Immunol Immunother* 2010; **59**:1163-1171.
16 Zhang G, Xu Y, Lu X, *et al.* Diagnosis value of serum B7-H3 expression in non-small cell lung cancer. *Lung Cancer* 2009; **66**:245-249.
17 Zang X, Thompson RH, Al-Ahmadie HA, *et al.* B7-H3 and B7x are highly expressed in human prostate cancer and associated with disease spread and poor outcome. *Proc Natl Acad Sci USA* 2007; **104**:19458-19463.
18 Martin-Orozco N, Muranski P, Chung Y, *et al.* T helper 17 cells promote cytotoxic T cell activation in tumor immunity. *Immunity* 2009; **31**:787-798.
19 Gabrilovich DI, Nagaraj S. Myeloid-derived suppressor cells as regulators of the immune system. *Nat Rev Immunol* 2009; **9**:162-174.
20 Dezfouli S, Hatzinisiriou I, Ralph SJ. Enhancing CTL responses to melanoma cell vaccines *in vivo*: synergistic increases obtained using IFNgamma primed and IFNbeta treated B7-1+ B16-F10 melanoma cells. *Immunol Cell Biol* 2003; **81**:459-471.
21 He L, Hakimi J, Salha D, Miron I, Dunn P, Radvanyi L. A sensitive flow cytometry-based cytotoxic T-lymphocyte assay through detection of cleaved caspase 3 in target cells. *J Immunol Methods* 2005; **304**:43-59.
22 Sznol M, Chen L. Antagonist antibodies to PD-1 and B7-H1 (PD-L1) in the treatment of advanced human cancer--response. *Clin Cancer Res* 2013; **19**:5542.
23 Hashiguchi M, Kobori H, Ritprajak P, Kamimura Y, Kozono H, Azuma M. Triggering receptor expressed on myeloid cell-like transcript 2 (TLT-2) is a counter-receptor for B7-H3 and enhances T cell responses. *Proc Natl Acad Sci USA* 2008; **105**:10495-10500.
24 Chen JT, Chen CH, Ku KL, *et al.* Glycoprotein B7-H3 overexpression and aberrant glycosylation in oral cancer and immune response. *Proc Natl Acad Sci USA* 2015; **112**:13057-13062.
25 Crispen PL, Sheinin Y, Roth TJ, *et al.* Tumor cell and tumor vasculature expression of B7-H3 predict survival in clear cell renal cell carcinoma. *Clin Cancer Res* 2008; **14**:5150-5157.
26 Roth TJ, Sheinin Y, Lohse CM, *et al.* B7-H3 ligand expression by prostate cancer: a novel marker of prognosis and potential target for therapy. *Cancer Res* 2007; **67**:7893-7900.
27 Sun Y, Wang Y, Zhao J, *et al.* B7-H3 and B7-H4 expression in non-small-cell lung cancer. *Lung Cancer* 2006; **53**:143-151.
28 Zang X, Sullivan PS, Soslow RA, *et al.* Tumor associated endothelial expression of B7-H3 predicts survival in ovarian carcinomas. *Mod Pathol* 2010; **23**:1104-1112.
29 Castriconi R, Dondero A, Augugliaro R, *et al.* Identification of 4Ig-B7-H3 as a neuroblastoma-associated molecule that exerts a protective role from an NK cell-mediated lysis. *Proc Natl Acad Sci USA* 2004; **101**:12640-12645.
30 Liu D, Bryceson YT, Meckel T, Vasiliver-Shamis G, Dustin ML, Long EO. Integrin-dependent organization and bidirectional vesicular traffic at cytotoxic immune synapses. *Immunity* 2009; **31**:99-109.
31 Liu D, Peterson ME, Long EO. The adaptor protein Crk controls activation and inhibition of natural killer cells. *Immunity* 2012; **36**:600-611.

(**Supplementary information** is linked to the online version of the paper on the *Cell Research* website.)